THE ASTROPHYSICAL JOURNAL, 246:193–202, 1981 May 15

ON THE RELATIONSHIP BETWEEN CORONAE AND MASS LOSS IN LATE-TYPE STARS

L. HARTMANN[1], A. K. DUPREE[1], AND J. C. RAYMOND[1]
Harvard-Smithsonian Center for Astrophysics
Received 1980 August 25; accepted 1980 November 19

ABSTRACT

We examine the temperature stratification of the wind of the hybrid atmosphere star α TrA (K4 II) by means of high-dispersion spectra taken with the *International Ultraviolet Explorer* satellite. C IV emission is shown to have a line width ~150–200 km s^{-1}, with Si III and C III exhibiting 100 km s^{-1} widths. Thus the "transition region" line emission in this hybrid star arises under conditions substantially different from the solar transition region. We suggest that the line widths reflect wind expansion, with C IV formed in an extended region flowing near the wind terminal velocity of 85 km s^{-1}. At large distances from the star, the wind cools and recombines to form a circumstellar shell visible in Mg II absorption.

We apply the stellar wind theory of Hartmann and MacGregor, in which the schematic dissipation of Alfvén waves drives the outflow in addition to heating the wind. It is shown that the stratification of temperature with velocity predicted by this theory can account for the observed line widths.

These observations of the warm, expanding corona in α TrA suggest a continuous progression between the high-temperature, low-mass-flux solar wind and the winds of luminous cool stars.

Subject headings: stars: chromospheres — stars: coronae — stars: late-type — stars: mass loss — ultraviolet: spectra

I. INTRODUCTION

Mass loss from late-type stars has been viewed in the past mainly from the perspective of the coolest, most luminous objects. Those stars which have the largest mass loss rates possess cold circumstellar shells expanding at velocities much less than the surface escape velocity. The contrast of these winds to the solar wind has led naturally to the supposition that the two types of mass loss have nothing to do with each other. However, recent ultraviolet observations (Hartmann, Dupree, and Raymond 1980) have shown that stars with "hybrid" winds exist. Such stars exhibit solar transition region lines such as N V and C IV, indicating gas of temperatures up to 2×10^5 K, with roughly solar emission measures $\int Ne^2 dh$; at the same time, Mg II and Ca II observations show the presence of cold circumstellar shells at moderately fast velocities ~50–100 km s^{-1}. The combination of solar type and supergiant type gas temperatures, with expansion velocities intermediate between that of the solar wind and cool luminous stellar winds, suggests a closer connection between the two types of mass loss than previously thought.

In this paper we discuss ultraviolet spectra of the hybrid atmosphere star α TrA (=HD150798; K4 II) first observed by Carpenter and Wing (1979) with *IUE*. Our purpose is to analyze the temperature stratification of the wind by investigating the velocity shifts of the emission lines obtained at high dispersion, and to examine the implications of such temperature structures for theories of mass loss and coronal formation.

II. OBSERVATIONS

IUE observations of α TrA were obtained on 1980 April 13. Details of the instrument may be found in Boggess *et al.* (1978). Spectra were obtained in the large aperture using both short and long wavelength cameras. The low dispersion spectrum between 1200 and 1900 Å shown in Figure 1 is very similar to the spectrum reported by Carpenter and Wing (1979) and to the spectra of α Aqr and β Aqr previously reported by Hartmann, Dupree, and Raymond (1980). Both low-temperature ions, such as S I, and high-temperature ions like N V, C IV, and Si IV are present. Line fluxes obtained from the low-dispersion spectrum are given in Table 1.

The Mg II *h* and *k* observations made at high dispersion are shown in Figure 2. The profile shows two absorption components whose minima are shifted by −13 km s^{-1} and −84 km s^{-1} relative to the star; we

[1]Guest Investigator with the *International Ultraviolet Explorer* satellite, which is sponsored and operated by the National Aeronautics and Space Administration, by the Science Research Council of the United Kingdom, and by the European Space Agency.

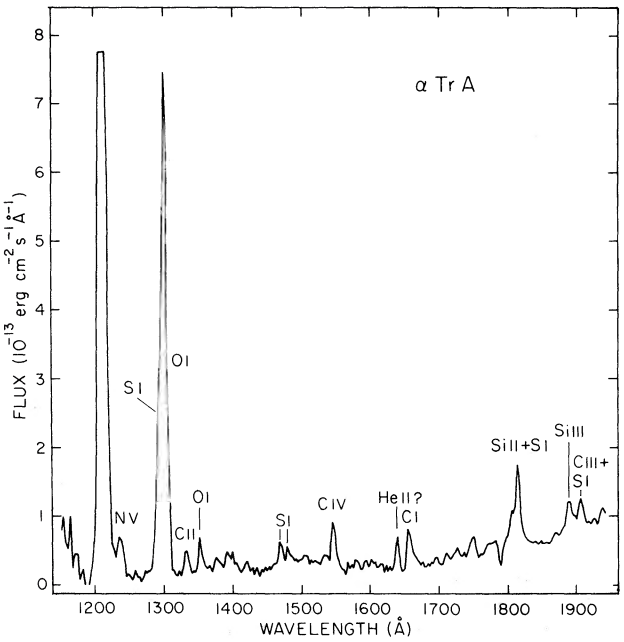

FIG. 1.—Low dispersion spectrum of α TrA, SWP 8570. Prominent emission features are marked. Note the asymmetry of the O I λ1300 line showing the presence of S I emission, confirmed by the high dispersion spectrum.

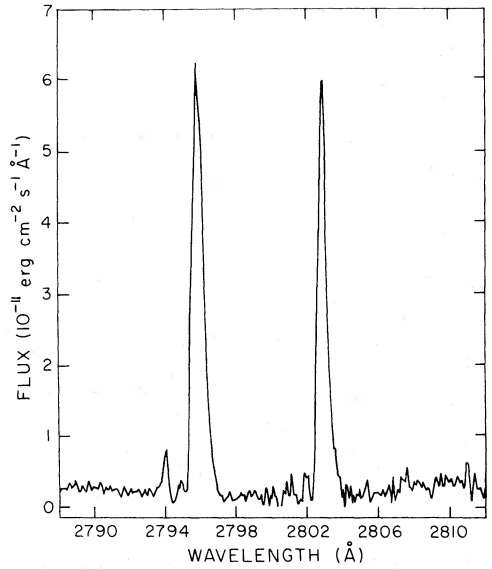

FIG. 2.—High dispersion Mg II spectra of α TrA. Two absorption components can be seen, one shifted by −13 km s^{-1} relative to the star, the other shifted by −84 km s^{-1}.

interpret the second of these as the terminal velocity of the stellar wind. The long wavelength spectrum and the low-dispersion, short-wavelength spectrum exhibited are similar to those measured earlier by Carpenter and Wing (1979) and indicate no fundamental change between 1979 February and 1980 April.

Figure 3 and Table 2 list information obtained from an 8 hour, high-dispersion exposure, taken just before the low-dispersion short-wavelength spectrum. In Figure 3*a* both O I and S I emission lines are seen. The S I lines are resonantly pumped by O I λ1302 emission. The indicated S I line which is missing (λ1303.11) is that member of the multiplet which cannot be resonantly pumped by fluorescence with O I. This confirms the suggested identification of S I at low dispersion by

TABLE 1

α TRIANGULI AUSTRALIS LINE FLUXES, LOW DISPERSION, SWP 8570

λ (Å)	Ident.	$F_\oplus$ [a]	$F_\star$ [b]	$F_\star/F_\odot$
1237	N V	~2.9	3.3+2	0.4
1303	O I+S I	>68	>7.6+3	>1.9
1333	C II	2.5	2.8+2	0.06
1352	O I	3.1	3.5+2	1.0
1391, 1399 ...	Si IV	3.7	4.1+2	0.16
1468	S I	3.0	3.4+2	
1482	S I	2.6	2.9+2	
1545	C IV	4.7	5.3+2	0.09
1639	He II, O I, S I	1.9	2.1+2	0.16
1656	C I	4.3	4.8+2	0.09
1750	...	2.4	2.7+2	
1795–1827 ...	Si II+S I	13.9	1.55+3	0.10
1892	Si III	2.9	3.3+2	
1900	S I	1.0	1.1+2	
1909	C III	2.3	2.6+2	
1914[c]	S I	1.5	1.7+2	

[a] Fluxes observed at Earth in 10^{-13} ergs cm^{-2} s^{-1}.
[b] Stellar surface fluxes in ergs cm^{-2} s^{-1}.
[c] Estimated from high dispersion spectrum.

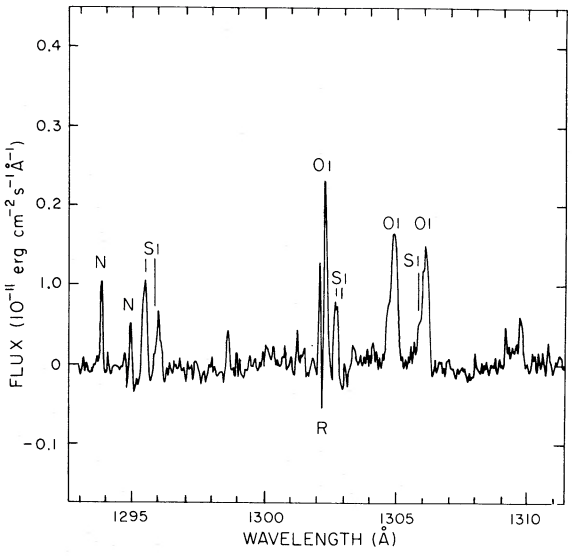

FIG. 3*a*

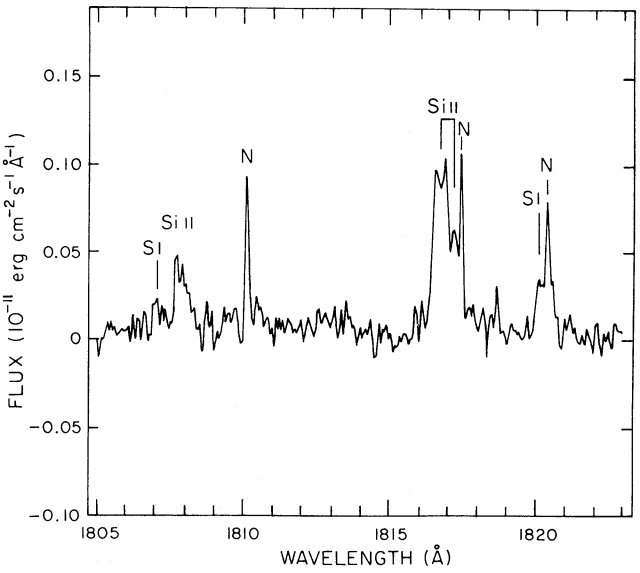

FIG. 3*b*

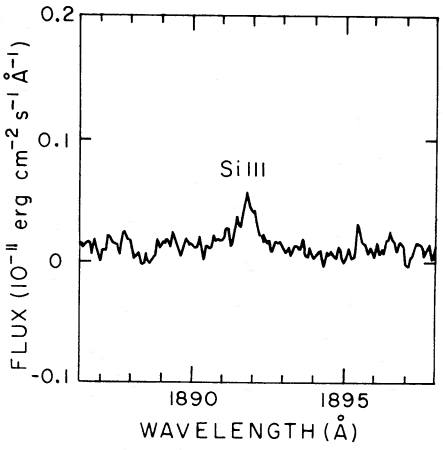

FIG. 3*c*

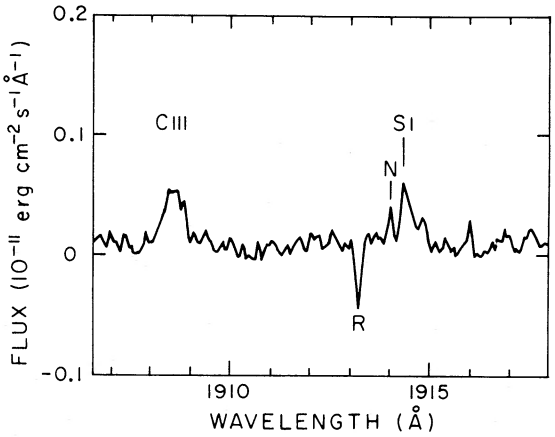

FIG. 3*d*

FIG. 3.—High dispersion spectra of α TrA in the short wavelength region. N is used to mark radiation noise spikes, and R is used for camera reseau marks. (*a*) Portion of the high-dispersion spectrum showing O I λ1302.17, λ1304.86, λ1306.03, and S I λ1295.65, λ1296.17, λ1302.34, λ1302.86, and λ1305.88. The S I member of multiplet 9 at λ1303.11 is not present because its upper level is not resonantly fluorescent with O I (Brown and Jordan 1980). (*b*) Spectrum showing Si II λ1808.01, λ1816.93 (apparently centrally reversed), λ1817.45, and S I λ1820.34, and possibly also λ1807.31. (*c*) High dispersion Si III λ1892.03 profile. (*d*) High dispersion C III λ1908.73 and S I λ1914.70 profiles.

Hartmann, Dupree, and Raymond (1980) and the suggestion of resonance fluorescence by Brown and Jordan (1980). O I itself is resonantly pumped by Lβ (Haisch *et al.* 1977).

The velocity widths and velocity shifts are given in Table 2 for each line. The derivation of these quantities deserves some comment. Because the exposure was taken in the large aperture, there is the possibility of a zero-point shift in the wavelength scale, depending upon where the object was centered in the aperture. We have adopted a zero-point shift defined by the mean of the Si, Si II, Si III, and C III lines. The standard deviation about the mean of the 10 lines is 6 km s^{-1}, which is a reasonable error given the resolution of about 30 km s^{-1} in the large aperture and signal-to-noise ratios for the individual line profiles.

This adopted zero-point shift results in an apparent redshift of 45 km s^{-1} for O I (Fig. 3*a*). However, this redshift is probably not real. Recall that the Mg II line has strong absorption components at −13 and −84 km s^{-1}. These components are so strong that it is likely that similar absorption components exist in O I, given the

TABLE 2

HIGH DISPERSION RESULTS, SWP 8569

Ion	λ (Å)	FW[a] (km s^{-1})	FWHM (km s^{-1})	$(V-V_*)$ (km s^{-1})
O I	1304.86	122	71	+45[b]
	1306.03	122	62	+47[b]
S I	1295.65	74	51	0
	1296.17	102	51	−3
	1302.86	71	51	0
	1900.29	66	32	+2
	1914.70	72	30	−13
Si II	1808.01	96	73	+7
	1816.92	[c]	...	+6
	1817.20	...	...	−1
Si III	1892.03	150	97	−5
C III	1908.73	132	94	+8
C IV.....	1549.19	...	150–200[d]	
	1550.77			
Mg II *k* ...	2795	...	...	−84, −13

[a] Measured at "base of line."
[b] See discussion in text; apparent redshift most probably caused by absorption.
[c] True width obscured by radiation noise spike.
[d] See text.

similar ionization potentials and relative abundances of these two ions. The presence of blue shifted absorption is made more plausible from inspection of the asymmetries shown in Figure 3*a*. The extent of the absorption is much more difficult to observe in O I than in Mg II, due to the relative narrowness of the O I emission component.

The derivation of the C IV line widths was difficult because these lines are extremely underexposed (Fig. 4 [Pl. 3]). The standard data reduction procedure does not clearly exhibit these lines, owing to problems such as radiation noise spikes being averaged into the interorder background. We have attempted to estimate the line width in two ways. One is to make an estimate from the two-dimensional image. The faintness of the lines prohibits an accurate determination of the line centers; however, we find that the emission is centered at the correct wavelengths for C IV to better than 0.3 Å. The other method uses the C IV flux observed in the 1 hour low-dispersion exposure which immediately followed the high-dispersion spectrum. We assume that the line flux did not change between exposures; this seems reasonable since the flux also agrees well with the spectrum taken about 1 year earlier by Carpenter and Wing (1979). By identifying the maximum excursion in the flux given by the standard Goddard data reduction at the appropriate wavelengths as an upper limit, and comparing this with the known line fluxes, one may derive a lower limit to the FWHM of the lines. In this we have used the calibration between low-dispersion and high-dispersion sensitivity derived by Cassatella, Ponz, and Selvelli (1980). The first method yields an estimated FWHM of 200 km s^{-1}; the second yields a FWHM $\gtrsim$150 km s^{-1}.

The Lα profile clearly exhibits blueshifted absorption. This line is not well exposed in our spectrum, so we defer a careful analysis for a subsequent paper in which we shall add spectra to improve the signal-to-noise ratio. For present purposes we simply note that the velocity shift of the absorption is $\sim -85 \pm 20$ km s^{-1}, with a column density $\sim 2 \times 10^{19}$ cm^{-2}. Some of this absorption may be interstellar, but the large velocity shift suggests that it arises mostly from the wind.

The line widths derived for C IV and for C III λ1909 and Si III λ1892 clearly indicate a situation far removed from solar transition region conditions. Very large turbulent velocities would be required to account for these widths and would dominate the gas pressure. However, the correspondence of the half-widths of the CIV lines with the wind terminal velocity indicated by the Mg II lines suggests that the broadening of C IV reflects wind expansion. While alternative explanations of the line widths which invoke "turbulence" cannot be ruled out, we prefer the wind hypothesis for simplicity. It is known that late type stars of very low gravity, with slow winds, exhibit expansion in chromospheric lines formed below $\sim 1 \times 10^4$ K (Goldberg 1979). It therefore seems reasonable to suppose that stars of somewhat higher gravity, with wind speeds intermediate between the slow supergiant flows and the solar wind, exhibit expansion in lines formed at intermediate ($\sim 10^5$ K) temperatures.

We interpret the results of Table 2 to yield the following picture of the wind of α TrA. The O I and S I

emission is formed near the star at low velocities. The λ1300 lines of S I may be broadened slightly by optical depth (Brown and Jordan 1980). The λ1900 S I lines are nearly as narrow as the expected instrumental width for large aperture exposures. Mg II absorption continues out to a velocity of ~ -15 km s^{-1}, at which point it ionizes due to the temperature rise ($T \gtrsim 1 \times 10^4$ K). (We attribute the low-velocity absorption to stellar rather than interstellar components since -20 km s^{-1} components are seen in several different stars; cf. Hartmann, Dupree, and Raymond 1980.) Assuming the Si III, C III, and C IV lines are not very optically thick, we infer expansion velocities from the line half-widths of $V \sim 45$ km s^{-1} at temperatures ~ 4–6×10^4 K, and $V \sim 100$ km s^{-1} at temperatures ~ 1 to 2×10^5 K. At large distances from the star, the gas cools sufficiently that Mg II once again becomes the dominant stage of ionization; this accounts for the second absorption component at -84 km s^{-1}, with a similar velocity in Lα.

III. DISCUSSION

a) *Nature of the α TrA Corona*

These results clearly show that the ultraviolet "transition region" lines observed in α TrA, and by implication in the other hybrid atmosphere stars, are formed under physical conditions greatly different from those in the Sun. The suggested expansion of 10^5 K gas at nearly terminal velocity indicates something more like a cool version of the solar corona. However, an explanation of the mass loss in terms of Parker-type thermal wind would require gas temperatures $T \gtrsim 4.6 \times 10^5$ K near the stellar surface (cf. Parker 1963). The interpretation of Si III and C III line widths indicates that expansion is well under way at much lower temperatures. The low-velocity Mg II component at 13 km s^{-1} suggests that expansion begins in the chromosphere, as observed in other stars with circumstellar shells (Goldberg 1979). It appears that the wind cannot be dominated by thermal expansion.

The circumstellar shell absorption in Mg II shows that the wind density is sufficiently large that the gas ultimately cools and recombines, in contrast to the solar wind. This suggests that solar-type coronal heating is present, but that the enhancement of radiative cooling at high densities prevents very high temperatures from being achieved—at least with a large emission measure. Although we have no direct measurement of gas at temperatures greater than 2×10^5 K, the λ1640 emission from He II can be used to place an upper limit on the high temperature ($\gtrsim 10^6$ K) emission measure, assuming that this line arises from recombination following X-ray photoionization (cf. Hartmann, Dupree, and Raymond 1980). We can derive only an upper limit to the He II flux from the low-dispersion spectrum. Brown and Jordan (1980) have shown that a narrow emission line occurs near λ1641.3 in a cool giant star; they suggest that this accounts for most of the λ1640 flux at low dispersion, and tentatively identify the line with either S I or O I. We find a similar result, although we are unable to rule out the possibility of a broad He II λ1640 component (FWHM ~ 100 km s^{-1} or greater) with less than 30% of the total low dispersion flux. This yields an emission measure limit $n_e^2 h \lesssim 10^{26}$ cm^{-5} according to the prescriptions of Hartmann, Dupree, and Raymond (1980), which is only about 3 times larger than the N V emission measure.

From inspection of Table 1, we see that the line surface fluxes are generally about 10^{-1} of solar values, except for N V, which is enhanced in its ratio to the solar N V emission by a factor of 4 relative to the other lines. This relative behavior of N V is similar to the situation in the other hybrid stars α Aqr and β Aqr (Hartmann, Dupree, and Raymond 1980), and suggests that the emission measure distribution may be peaking at a few times 10^5 K. Similarly, the upper limit to the 10^6 K gas from the He II λ1640 upper limit indicates a slower rise in emission measure with increasing temperature than in the Sun. These indications, coupled with the observation of C IV–emitting gas expanding near the wind terminal velocity, may mean that the peak coronal temperature for α TrA is less than 10^6 K; such low-temperature coronae for low-gravity stars have been suggested by Weymann (1962) and Parker (1963). The column densities of cool gas overlying a possible corona are $\lesssim 10^{20}$ cm^{-2} (see the wind models below), so that X-ray emission from a possible hot corona at energies greater than $\frac{1}{4}$ keV will not be appreciably absorbed. X-ray observations should therefore provide an unambiguous test for hot coronal meterial.

The short cooling times of the wind material (estimated below) clearly point to a continuing supply of mechanical energy which keeps the gas at $\sim 10^5$ K at large distances from the stellar surface. This again is much different from the solar situation, where many authors have emphasized that the bulk of solar coronal emission occurs in regions of closed magnetic fields (cf. Rosner, Tucker, and Vaiana 1978). We infer that the "coronal" heating in hybrid stars like α TrA probably occurs in magnetically open regions because of the large expansion velocities detected. Such behavior does have a solar precedent. It has been known that some source of energy and/or momentum must be added to the solar wind at distances of several solar radii (Munro and Jackson 1977); Alfvén waves have been suggested to be the responsible agent (Hollweg 1973; Jacques 1977, 1978). It is also known that conduction is not sufficient to balance the energy losses in coronal hole transition regions, so that some heating mechanism must be present (Munro and Withbroe 1972).

b) *The Connection between Coronal Heating and Momentum Deposition*

The presence of coronal heating in regions where significant wind acceleration is taking place suggests

that the two effects are related, even if the wind is not driven by thermal expansion. Hartmann and MacGregor (1980) have developed a theory of mass loss in late-type stars in which the Alfvén waves thought to be important in the acceleration of the solar wind are invoked to drive the outflows of luminous cool stars as well. The crucial point is that the waves must be dissipated over a distance comparable to a stellar radius in order to achieve terminal velocities comparable to those observed. The theory is schematic in that the dissipation (e-folding) length scale L_D is parametrized as $L_D = R_\star$ because of the very great uncertainties in calculating the damping rates. Similarly, the actual wave fluxes and stellar surface magnetic fields are unknown. The strength of the theory is that, for a given mass loss rate $\dot{M}$ controlled by the wave flux F, and for a given terminal velocity V_∞ controlled by L_D, the local heating rate F/L_D is specified. With an estimate of the radiative cooling law, the temperature structure predicted to accompany a given wind model can be computed.

c) *Wind Model Calculations*

We are now able to compare our observations with sample wind models calculated using the Alfvén wave–driven wind theory of Hartmann and MacGregor (1980). A full description of the wind equations is given in that paper; here we simply sketch the principal assumptions made in calculating the winds. The wind theory in its present crude state assumes an isothermal, low-temperature wind for calculating the velocity profile. This assumption does not affect the wind structure significantly unless the temperature implied by the heating approaches the thermal wind temperature $T_W = GM/2Rr$, where R is the gas constant. In general Hartmann and MacGregor found this condition to be satisfied for their models with low stellar gravities. Models for K–M supergiants indicated heating resulting in warm chromospheres at temperatures $\sim$5000–10,000 K, extending over a few stellar radii from the surface. However, the temperatures in the extended heating region increase with increasing stellar surface gravity. For $\log g > 2$, wave energy dissipation over $L_D \sim R_\star$ does not result in cool, low-velocity winds, but in high-temperature ($>10^5$ K) coronae. Since the hybrid stars are found near the supersonic transition locus (STL) (Mullan 1978), the locus in the H-R diagram where optical circumstellar lines first make their appearance (Reimers 1977), and where $\log g \sim 1$–2, it is possible to use the Hartmann and MacGregor theory to construct wind models which have gas at temperatures $\sim 1 \times 10^5$ K in their expanding winds.

In order to calculate a wind model we need to define appropriate stellar parameters. This is somewhat difficult because of the confusion in spectral type. Carpenter and Wing (1979) point out that the k_1 width of Mg II is much wider than is consistent with the assignment of luminosity class III, and that the star should be reclassified as II or Ib. We measure a full width of approximately 3.15 Å for Mg II; using the relation in Dupree (1976) between M_v and line widths through a Wilson-Bappu effect, $M_v \sim 3.1$. This results in a distance of 100 pc. From the Barnes-Evans (1976) relation for $B-V$ and the angular diameter, we derive a radius $\sim 260\ R_\odot$. Alternatively, the trigonometric parallax distance of 42 pc yields a radius $\sim 110\ R_\odot$ from the angular diameter.

Because of the uncertainty in luminosity class the surface gravity is not well known. Hartmann and MacGregor (1980) showed that observed stellar wind terminal velocities are consistent with models in which the waves have a damping length of about one stellar radius. Adopting these values for L_D results in terminal velocities ~ 80 km s^{-1} for $(M/M_\odot)(R_\star/R_\odot)^{-1} \sim 0.1$. Such a ratio is consistent with a K4 II spectral type. Models with constant $M/R_\star$ and constant surface parameters have the same velocity distributions as a function of $r/R_\star$.

Setting $M/R \sim 0.1(M_\odot/R_\odot)$, we have models with terminal velocities ~ 80 km s^{-1}. Choosing an initial wave flux and reference level density then permits us to calculate an isothermal wind model. We can show from *a posteriori* inspection of the terms in the energy equation that wave dissipation heating and radiative cooling are the dominant terms in the energy equation, except at very large distances from the star. Thus, a local gas temperature can be estimated by balancing heating with radiative cooling,

$$F/L_D \sim \Lambda(T) N_e N_{\rm H}, \qquad (1)$$

where F is the local wave flux at r, N_e and $N_{\rm H}$ are the electron and hydrogen number densities, and $\Lambda(T)$ is a radiative cooling law which is formally only a function of T, but in reality must include optical depth effects. We use the results of Hartmann and MacGregor (1980) to compute $\Lambda(T)$ in the range 8000 K $\lesssim T \lesssim$ 23,000 K. At higher temperatures we use the optically thin cooling law of Raymond as parametrized by Rosner, Tucker, and Vaiana (1978).

The models calculated in such a way are schematic. No provision is made for the undoubted nonradial character of the magnetic fields. Similarly, the dissipation processes are parameterized crudely by the damping length fixed to equal the stellar radius. The wave fluxes and magnetic fields are unknown, chosen to match observational quantities such as the wind emission measure. Our purpose in constructing such models is simply to investigate in a quantitive way the possible connection between the energy deposition mechanism which heats the wind and the momentum deposition mechanism which drives the outflow.

In addition to the schematic nature of the calculations, we point out some simplifying approximations

which do not always strictly hold. One is the assumption that the velocity structure can be calculated by initially assuming a cold, isothermal flow, in this case at 10^4 K. The approximation is good as long as the gas temperature is much less than T_W. This condition is satisfied in the present models except in the region ~ 2.5–4 $R_\star$. This far from the star the wind is at nearly terminal velocity, and by keeping the wind temperature below T_w we do not expect major changes in the velocity profile.

The other important approximation is the neglect of certain terms in the energy equation. At large distances the expansion terms are not negligible when compared with the radiative cooling law; and the cooling law for temperatures $\lesssim 1\times10^4$ K is more appropriate for high-density, optically thick chromospheric regions. More serious is the neglect of conduction. The N v emission clearly indicates the presence of gas at temperatures greater than 8×10^4 K. However, with the radiative cooling law from Rosner, Tucker, and Vaiana (1978), one cannot determine a stable temperature greater than this in the absence of conduction. As Rosner and Vaiana (1977) have shown, the calculation of coronal-type heating in an expanding atmosphere, including conductive flux, is a complicated problem, difficult to solve in any but the simplest geometries and physical conditions, and is beyond the scope of the present discussion. We simply limit ourselves to a crude estimate of the amount of coronal emission that might arise from regions at $T>8\times10^4$ K.

Despite these approximations, these wind models are quantitatively useful, for they enable us to calculate emission measures for all but the hightest excitation lines, and to predict the velocity widths in the lines of the observed ions. This is sufficient for a preliminary exploration, given the limited amount of information available from the data on the physical conditions in the wind.

d) Comparison of Models with Observations

In Tables 3 and 4 we list two wind models computed under the assumptions detailed above. The models have similar velocity and temperature structures, differing primarily in their mass loss rates and emission measures. Model A matches the line fluxes of the hybrid star β Aqr best; model B, with smaller emission measures, is closer to the low surface fluxes of α TrA. The temperature structures have been carefully adjusted to avoid temperatures 8×10^4 to 2×10^5 K. Otherwise, as noted above, one would have to include the conductive flux, and the neglect of thermal expansion would be more serious.

The line fluxes have been computed using emissivity calculations for $N_eT=10^{12}$ using the ionization balance calculations of Raymond and Doyle (1980). The generally small temperature gradients in the models indicate that ionization equilibrium is a good approximation. The temperature of formation of Si III is uncertain, owing to charge exchange (Baliunas and Butler 1980); we adopt a very rough estimate of $T_{\max}\sim4\times10^4$ K. Similarly, on the basis of radiative transfer calculations, we adopt a temperature $\sim$8000–9000 K for the disappearance of Mg II absorption (Baliunas and Avrett, private communication).

With this information, we can make the following comparisons between the models and observations listed

TABLE 3

WIND MODEL A[a]

Z	V (km s^{-1})	N_T (cm^{-3})	F_W (ergs cm^{-2} s^{-1})	log $\Lambda(T)$	$T/10^3$ K
1.00 ...	1.04	1.67+9	5.11+5	−25.14	<7
1.20 ...	14.5	8.32+7	2.75+5	−22.80	15
1.50 ...	39.9	1.93+7	1.25+5	−21.88	41
1.73 ...	55.6	1.04+7	7.22+4	−21.58	55
2.02 ...	71.0	5.99+6	3.79+4	−21.38	68
2.32 ...	82.6	3.91+6	2.04+4	−21.28	72
2.62 ...	91.0	2.78+6	1.14+4	−21.23	76
2.92 ...	96.9	2.10+6	6.55+3	−21.23	76
3.22 ...	101	1.66+6	3.85+3	−21.21	78
3.52 ...	104	1.35+6	2.31+3	−21.26	74
4.12 ...	106	9.65+5	8.69+2	−21.43	62
4.72 ...	106	7.33+5	3.44+2	−21.60	54
5.62 ...	105	5.25+5	9.11+1	−21.88	41
6.52 ...	102	3.99+5	2.56+1	−22.08	28
8.02 ...	98.3	2.75+5	3.38	−22.75	16
10.12 ...	94.0	1.80+5	2.25−1	−23.56	11
11.92 ...	91.4	1.34+5	2.40−2	−24.27	7.8

[a] Model A parameters: $M=15.7\ M_\odot$, $R_\star=157\ R_\odot$, $B_0=2.7$ gauss, $L_D=R_\star$, $F_0=5.11\times10^5$ ergs cm^{-2} s^{-1}, $\dot{M}=4.3\times10^{-9}\ M_\odot$ yr^{-1}, $V_\infty=81.4$ km s^{-1}; $V_\infty=V(Z=150)$.

TABLE 4

WIND MODEL B[a]

Z	V (km s^{-1})	N_T (cm^{-3})	F_W (ergs cm^{-2} s^{-1})	log $\Lambda(T)$	$T/10^3$K
1.00 ...	5.82	1.00+8	9.53+4	−23.66	9.6
1.12 ...	16.5	2.81+7	6.59+4	−22.70	16
1.27 ...	30.4	1.19+7	4.29+4	−22.16	25
1.57 ...	53.5	4.41+6	1.98+4	−21.63	51
1.79 ...	66.7	2.77+6	1.19+4	−21.44	62
2.09 ...	79.9	1.67+6	6.21+3	−21.29	72
2.39 ...	89.0	1.14+6	3.40+3	−21.23	76
2.69 ...	95.1	8.46+5	1.92+3	−21.21	78
2.99 ...	99.1	6.57+5	1.12+3	−21.23	76
3.29 ...	102	5.27+5	6.69+2	−21.26	74
3.59 ...	103	4.38+5	4.05+2	−21.32	71
4.19 ...	103	3.22+5	1.55+2	−21.47	60
4.79 ...	102	2.49+5	6.23+1	−21.64	50
5.67 ...	99.4	1.82+5	1.72+1	−21.93	36
6.59 ...	96.3	1.39+5	4.88	−22.24	23
8.09 ...	91.8	9.69+4	6.66−1	−22.79	15
10.04 ...	87.4	6.60+4	5.60−2	−23.53	10.7
11.99 ...	84.3	4.80+4	5.13−3	−24.29	7.7

[a] Model B parameters; $M=27.7\ M_\odot$, $R_\star=277\ R_\odot$, $B_0=0.8$ gauss, $L_D=R_\star$, $F_0=9.53\times10^4$ ergs cm^{-2} s^{-1}, $\dot{M}=4.76\times10^{-9}\ M_\odot$ yr^{-1}, $V_\infty=73.5$ km s^{-1}.

in Tables 5 and 6. The line widths are given in two ways. The first value given is the line width due solely to expansion; the second value, listed in parentheses, includes the rms radial velocity amplitude of the propagating Alfvén waves, which is $\sim$50 km s^{-1} in model B for the region of interest. In either case we find reasonable agreement between the model emission line widths and the observations.

Brown and Jordan (1980) have shown that values of the ratio of λ1914.68 to λ1900.27 less than 3.5 to 1.0 suggest that the lines are optically thick, so $\int N(\text{S I})dl\sim 10^{16}$ cm^{-2}; this condition appears to apply to α TrA. If we estimate the density length scale as the isothermal, hydrostatic density scale height for model B, then we find $N_H\sim10^{10}$ cm^{-3} where the S I lines are formed. Given the wave flux and magnetic field adopted for model B, we predict an rms Alfvén wave amplitude$\sim\pm10$ km s^{-1}; this is small enough to be compatible with the observations. If the density where S I is formed is much lower, the wave amplitudes would be much larger, so there would be difficulty in reconciling the observed line widths with the predicted wave amplitudes.

It is clear that the Alfvén wave–driven wind models can account for the general temperature stratification with velocity in the wind of α TrA. The biggest deficiencies of model B are the lack of N V–emitting gas, and that the emission measures are too large. These problems are in fact related. It was not hard to find parameters such that the winds had smaller emission measures. However, reducing the wind density also tended to drive the heating rate above the plateau in the optically thin cooling law at 8×10^4 to 2.5×10^5 K, so that the model was not self-consistent in terms of the assumptions adopted here. In reality there is no reason why regions with temperatures greater than 8×10^4 K cannot occur in these winds at $r\sim2$–$3\ R_\star$, in which the divergence of the conductive flux balances the other terms in the energy equation. We argue that there is but

TABLE 5

COMPARISON OF WIND MODEL EMISSION WITH OBSERVATIONS

	MODEL A		MODEL B		
PARAMETER	C II	C IV	C II	CIII	C IV
F[a]	1.3×10^4	1.7×10^4	3.5×10^3	9.4×10^3	3.2×10^3
F/F_*[b]	4.1	2.5	13	34	6

[a] $F=L_{em}/4\pi R_\star{}^2$ in units of ergs cm^{-2} s^{-1}, where L_{em} is the total line luminosity.
[b] $F/F_*=F/F(\beta$ Aqr) for model A; $F/F_*=F/F(\alpha$ TrA) for model B.

TABLE 6

VELOCITY COMPARISONS BETWEEN MODEL B AND OBSERVATIONS OF α TRIANGULI AUSTRALIS

Feature	Model B[a]	Observed
Mg II CS velocities (km s^{-1}) ...	−4, −74	−13, −84
S I FWHM	(20)	$\lesssim$20[b]
Si III FWHM	∼80 (∼120)	97
C III FWHM	66 (115)	94
C IV FWHM	170 (194)	150−200

[a] Values in parentheses include turbulent broadening due to the propagating waves.

[b] Assuming instrumental resolution $R \sim 1.2 \times 10^4$.

a short step between model B and the actual situation in the wind of α TrA, in which a scaled emission measure $(\int N_e^2 dV)/$

The Mg II circumstellar equivalent widths are difficult to match for two reasons. First, the turbulent broadening is unknown. Observations of α Aqr (Dupree and Baliunas 1979) have shown changes in the CS equivalent widths over time scales of less than a year. This suggests that a large fraction of the line width may be due to variations in the wind terminal velocity. Second, the "inner shell" radius where Mg II recombines is not well defined in the models, both because neglect of expansion terms in the energy equation is no longer valid, and because our cooling law, derived for optically thick, dense chromospheric conditions, is probably not applicable.

We may make a crude comparison in the following way. The width of $\sim\pm 40$ km s^{-1} and depth of the Mg *k* circumstellar absorption component implies a minimum total hydrogen column density of $\sim 10^{18}$ cm^{-2}. Assuming the inner shell radius of model B is $\sim 12 R_\star$, the total column density would be $\sim 10^{19}$ cm^{-2}. Thus model B is compatible with observation in this regard, pending more accurate values of the turbulent velocity and cooling rates.

The model winds presented here are only schematic and do not satisfy all the observational constraints. However, they are able to explain the observed stratification of temperature and expansion velocity in the wind of α TrA, and make plausible the suggestion that coronal heating and mass loss may arise from the same mechanism. This should encourage further work on hybrid wind models which include a full energy equation, including thermal conduction.

IV. CONCLUSIONS

The hybrid atmosphere star α TrA exhibits broad C IV emission which we interpret as arising from a region expanding at nearly the terminal velocity of the wind. The emission measure of very high-temperature gas ($\gg 10^5$ K) is likely to be relatively small. We interpret this result not as a weakening of solar coronal type heating, but rather as the cooling effect of enhanced wind densities for mass loss rates much greater than that of the Sun. This interpretation can be tested by observations of X-ray emission from hybrid stars and by searches for a correlation between ultraviolet line widths and circumstellar shell velocities.

The high-dispersion observations of α TrA indicate the presence of a mechanism which continuously heats gas at appreciable distances from the star, in regions where the magnetic field configuration is probably open. This suggests that propagating waves are necessary to account for such heating. The possibility that the momentum carried by the waves can drive the outflow naturally arises. Using the wind theory of Hartmann and MacGregor (1980), we are able to demonstrate the plausibility of the Alfvén wave–driven wind hypothesis in an approximate but fairly quantitative fashion.

The Alfvén wave–driven wind theory was originally developed in order to account for mass loss from cool supergiants and the associated extended, warm chromospheres about such stars from the action of wave modes known to exist in the solar wind. Thus the hybrid atmosphere stars provide a crucial link between the activity of cool, luminous stars and solar behavior. The extended, expanding 10^5 K wind region falls in a natural sequence between the solar corona and extended chromospheres, with a continuous progression of decreasing "coronal" temperatures with decreasing stellar gravity.

We gratefully acknowledge the assistance of the *IUE* Observatory staff in the acquisition and reduction of these data. This work was supported by NASA grant NAG 5-87.

REFERENCES

Baliunas, S. L., and Butler, S. E. 1980, *Ap. J.(Letters)*, **235**, L45.
Barnes, T., and Evans, D. S. 1976, *M.N.R.A.S.*, **174**, 489.
Boggess, A., *et al.* 1978, *Nature*, **275**, 361.
Brown, A., and Jordan, C. 1980, *M.N.R.A.S.*, in press.
Carpenter, K. G., and Wing, R. F. 1979, *Bull. AAS*, **11**, 419.
Cassatella, A., Ponz, D., and Selvelli, R. L. 1980, preprint.

Dupree, A. K. 1976, in *Phys. des Mouvement dan les Atmos. Stellaires*, ed. R. Cayrel and M. Steinberg (Editions du C.N.R.S.), p. 439
Dupree, A. K., and Baliunas, S. L. 1979, *IAU Circ.*, No. 3435.
Goldberg, L. 1979, *Quart. J. R. A. S.*, **20**, 361.
Haisch, B. M., Linsky, J. L., Weinstein, A., and Shine, R. A. 1977, *Ap. J.*, **214**, 784.
Hartmann, L., Dupree, A. K., and Raymond, J. C. 1980, *Ap. J.(Letters)*, **236**, L143.
Hartmann, L., and MacGregor, K. B. 1980, *Ap. J.*, **242**, 260.
Hollweg, J. V. 1973, *Ap. J.*, **181**, 547.
Jacques, S. A. 1977, *Ap. J.*, **215**, 942.
Jacques, S. A. 1978, *Ap. J.*, **226**, 632.
Mullan, D. J. 1978, *Ap. J.*, **226**, 151.
Munro, R. H., and Jackson, B. V. 1977, *Ap. J.*, **213**, 874.
Munro, R. H., and Withbroe, G. L. 1972, *Ap. J.*, **176**, 511.
Parker, E. N. 1963, *Interplanetary Dynamical Processes* (New York: Interscience), pp. 256 ff.
Raymond, J. C., and Doyle, J. 1980, in preparation.
Reimers, D. 1977, *Astr. Ap.*, **57**, 395.
Rosner, R., Tucker, W. H., and Vaiana, G. S. 1978, *Ap. J.*, **220**, 643.
Rosner, R., and Vaiana, G. S. 1977, *Ap. J.*, **216**, 141.
Weymann, R. 1962, *Ap. J.*, **136**, 844.

A. K. DUPREE, L. HARTMANN, and J. C. RAYMOND: Center for Astrophysics, 60 Garden Street, Cambridge, MA 02138

PLATE 3

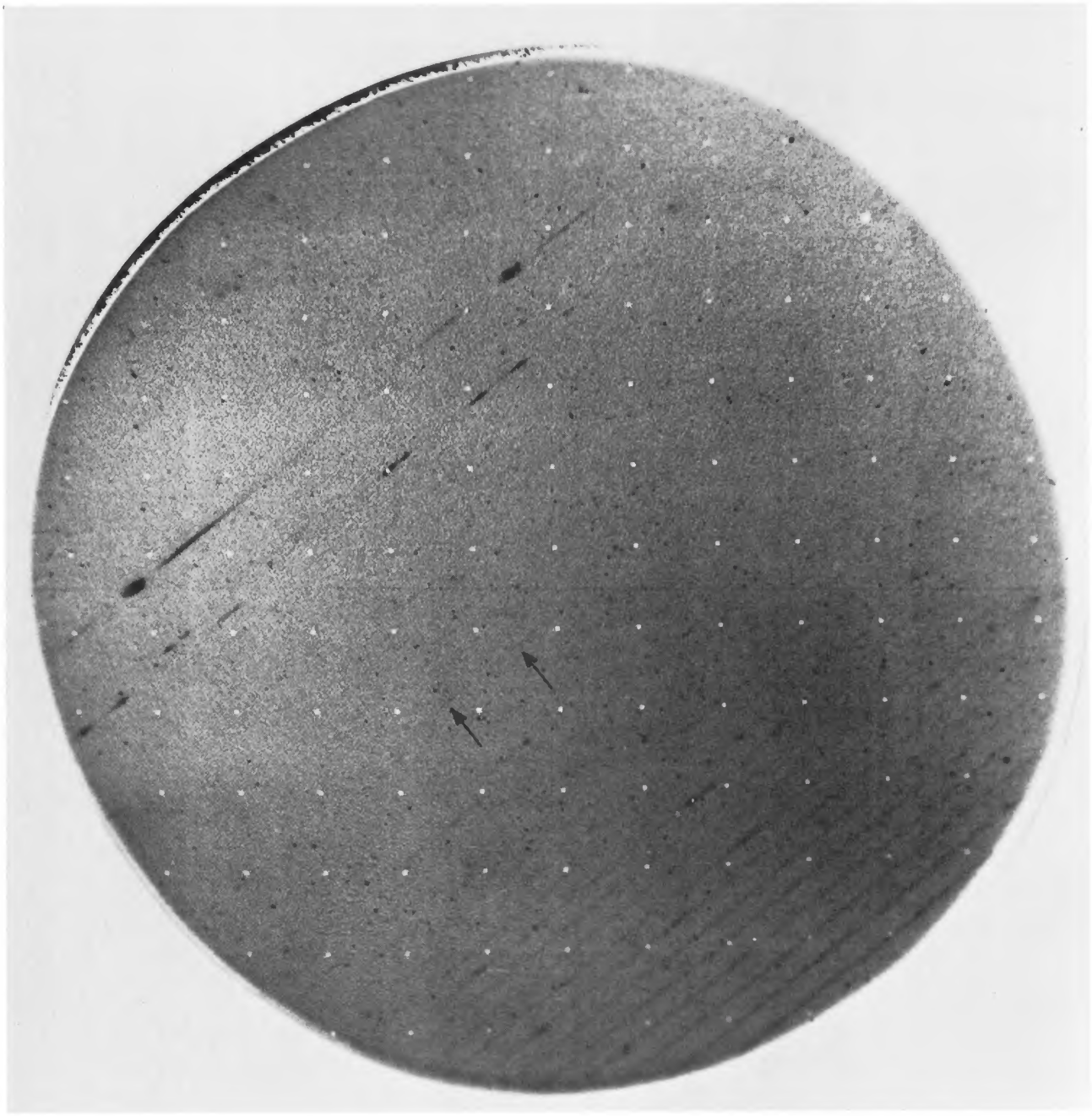

FIG. 4.—Image of SWP 8569, with broad C IV emission indicated